gases

MDPI

Article

Diagnosis of GHG Emissions in an Offshore Oil and Gas Production Facility

Victor Leonardo Acevedo Blanco [1] and Waldyr Luiz Ribeiro Gallo [2,*]

[1] Vanti Group, Bogotá 253448, Colombia; victorl_11_5@hotmail.com
[2] Energy Department, University of Campinas, Campinas 13083-860, Brazil
* Correspondence: gallo@fem.unicamp.br

Abstract: This work presents a diagnosis of greenhouse gas (GHG) emissions for floating production storage and offloading (FPSO) platforms for oil and gas production offshore, using calculation methodologies from the American Petroleum Institute (API) and U.S. Environmental Protection Agency (EPA). To carry out this analysis, design data of an FPSO platform is used for the GHG emissions estimation, considering operations under steady conditions and oil and gas processing system simulations in the Aspen HYSYS® software. The main direct emission sources of GHG are identified, including the main combustion processes (gas turbines for electric generation and gas turbine-driven CO_2 compressors), flaring and venting, as well as fugitive emissions. The study assesses a high CO_2 content in molar composition of the associated gas, an important factor that is considered in estimating fugitive emissions during the processes of primary separation and main gas compression. The resulting information indicates that, on average, 95% of total emissions are produced by combustion sources. In the latest production stages of the oil and gas field, it consumes 2 times more energy and emits 2.3 times CO_2 in terms of produced hydrocarbons. This diagnosis provides a baseline and starting point for the implementation of energy efficiency measures and/or carbon capture and storage (CCS) technologies on the FPSO in order to reduce CO_2 and CH_4 emissions, as well as identify the major sources of emissions in the production process.

Keywords: GHG emissions inventory; fugitive emissions; offshore oil and gas production; carbon sequestration in oil fields; power plant GHG emissions

Citation: Acevedo Blanco, V.L.; Gallo, W.L.R. Diagnosis of GHG Emissions in an Offshore Oil and Gas Production Facility. *Gases* **2024**, *4*, 351–370. https://doi.org/10.3390/gases4040020

Academic Editors: Cinzia Tornatore and Cherng-Yuan Lin

Received: 30 July 2024
Revised: 12 September 2024
Accepted: 29 September 2024
Published: 31 October 2024

1. Introduction and Objective

The oil and gas industry is one of the largest contributors to global carbon dioxide and methane emissions [1,2] due to the high energy intensity required in the production, refining, and transport processes of hydrocarbons, as well as the occurrence of greenhouse gas (GHG) escapes due to flaring and venting, in addition to emissions from combustion processes.

Oil and natural gas production in Brazil has been carried out in offshore installations in deep waters for many years [3]. More recently, production has moved to fields located not only in large water depths but also at great geological depths, the so-called "Pre-salt". Figure 1 shows the importance of this oil province for the country.

Oil and gas industry operations on offshore platforms, specifically on floating production storage and offloading (FPSO) units, present energy and environmental challenges to be studied in more detail due to the use of fossil fuels to obtain the needed energy independence for offshore installations. The use of fossil fuels induces GHG emissions into the atmosphere. To meet environmental commitments, oil companies have made efforts to measure and estimate pollutant emissions into the atmosphere. Various researchers [5–8] present energy and exergy analysis in offshore installations to study energy efficiency actions to mitigate the impact on the environment.

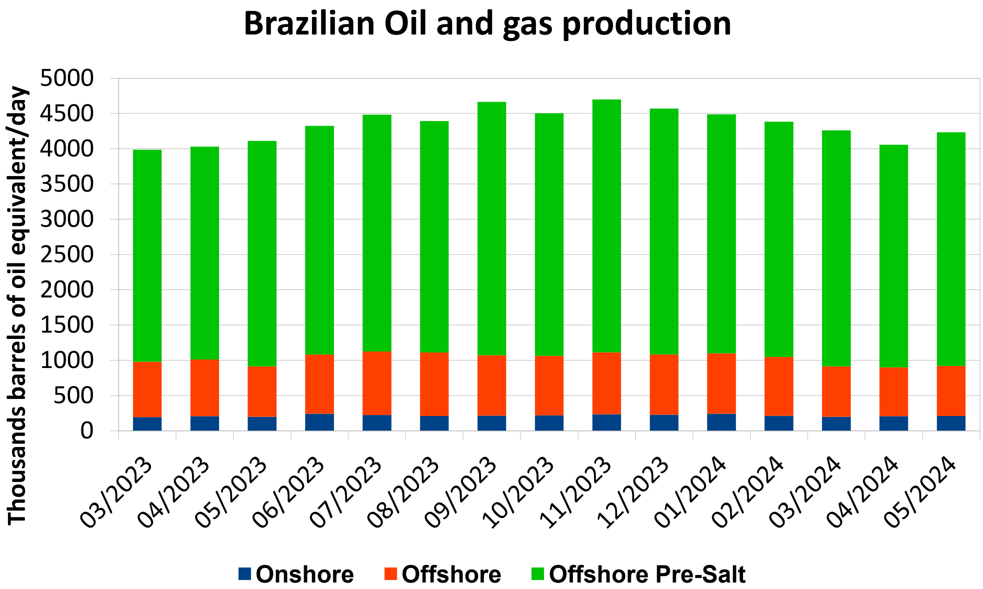

Figure 1. Oil and gas production in Brazil—2023/2024. Own preparation from data source: [4].

An important point to highlight is the notable predominance of oil and natural gas exploration and production activities in emissions, accounting, roughly speaking, for 90% of emissions from fuel production. This fact is not surprising, as the oil production and refining industry, as well as producing energy, is also a large consumer of energy.

The ratio of gas volume in the oil produced (GOR) under "standard" conditions is one of the most important parameters in a field's production strategy. High GOR values (high quantities of gas) lead to high production of natural gas, which can be used on platforms for energy requirements, used to increase oil production (gas-lift, reinjection), or sent for commercial exploitation on the market. During the lifetime of the oil field, the oil and gas properties vary and influence GHG emissions because, as the field becomes mature, oil and gas production decreases, decreasing energy demand in terms of hydrocarbon processing, but increasing in terms of water or gas injection as techniques to prolong production levels.

Pre-salt oil contains significant amounts of natural gas, with a high percentage of CO_2. There are uncertainties surrounding the volume of natural gas to be used for re-injection into the well, as well as the CO_2 produced from separation processes on the platforms, in order to maintain the reservoir pressure at an adequate level. For the commercial use of natural gas, the CO_2 molar fraction must be below 3%. Thus, the separation of CO_2 from the natural gas to be sold is expected. This separation process must still occur at the FPSO, and the CO_2-rich gas stream must be re-injected into the field, characterizing a CCS process.

The assessment and quantification of GHG emissions in industries are the first measures in emission reduction plans and implementation of energy efficiency measures [9,10]. The preparation of GHG emission inventories consists of quantifying polluting gases emitted or removed from the atmosphere over a period of time. Decision-makers, whether at government or corporate level, use inventories as a baseline for developing mitigation strategies and policies, in addition to evaluating such measures.

The main objective of this work is to diagnose GHG emissions from the oil and gas production and treatment process on a typical FPSO platform, used in pre-salt fields in ultra-deep waters in Brazil. To carry out the diagnosis in the most accurate way possible, it is necessary to identify each process involved in the production platform, considering not only combustion processes but also the practice of flaring, the existence of venting, and fugitive emissions in the oil production process and gas.

The scope of this diagnosis is specifically focused on the processes that occur on the topside of the FPSO during its operation and considers CO_2, CH_4, and N_2O as relevant GHG. Consolidated results are expressed in CO_2 equivalent emissions.

2. GHG Emissions from Offshore Oil Production, Including CCS

Several studies have been published on the need to reduce the carbon footprint in oil and gas production activities, especially for offshore conditions. The physical link between the consumption of fossil fuels on the platform and CO_2 emission levels indicates the need for efficiency gains in processes involving combustion. There is also the need to reduce the practice of flaring, which must be reduced to the minimum necessary for the safety of production operations.

Furthermore, offshore oil field is considered one of the places where CO_2 can be stored for a long time. The capture of CO_2 can occur in the oil production FPSO from combustion exhaust gases, from CO_2 present in the natural gas or captured elsewhere and transported to the oil field. In this sense, oil fields can be seen as part of the carbon capture and sequestration (CCS) studies.

The thermodynamic performance of oil and gas separation processes has been analyzed using the concepts of exergy and irreversibility. Silva and Oliveira Jr. [11] analyzed an FPSO platform similar to the one analyzed in this work. In addition to analyzing process efficiencies, the authors calculated CO_2 emissions arising from the electrical energy generation process by carbon mass balance between the fuel and combustion gases. The performances of different prime-movers were compared: gas turbines, combined cycles, and piston engines. The average emission of CO_2 for the natural gas ranges from 19.0 gCO_2/MJ to 19.8 gCO_2/MJ, depending on the cogeneration plant configuration, while it ranges from 19.4 gCO_2/MJ to 26.8 gCO_2/MJ for the oil.

Volsund et al. [12] analyze different options for energy supply for offshore oil production in the North Sea: the traditional use of natural gas produced in the field, hydrogen, ammonia, and biofuels supplied externally to the platform; offshore wind energy; and direct energy supply electricity for the FPSO. Each option is discussed considering its potential advantages and the risks involved. Furthermore, the paper also considers CCS options directly on the platform, through amine CO_2 absorption systems or employing oxy-fuel combustion technologies. The work emphasizes that the options with better performance in GHG still bring technological challenges or involve bulky equipment (FPSO has limitations in available area and weight) or can even pose new health safety concerns, especially in the case of using ammonia and hydrogen. The solutions with the best prospects in the short term consist of the combination of conventional generation complemented by offshore wind energy, the "power island" concept generating electrical energy in a high-efficiency combined cycle or even, whenever the distance from the coast allows, the import of electrical energy produced onshore by renewable sources.

The trade-offs between environmental performance and the economic costs of operating an FPSO were studied by Zuochao et al. [13] employing the LCA technique, considering the materials, the manufacturing of the installation, its operation, and decommissioning. Using a distributed generation system encompassing solar, wind, and natural gas energy, the authors developed an optimization with two objectives: maximum reduction in the carbon footprint and operating cost of the energy production system. Fixed emission factors were adopted, and the work did not consider the effect of the production curve over time. Pareto extremes indicate very high operating costs or a large carbon footprint. A combination of wind energy and natural gas (without the use of solar energy) can greatly reduce operating costs while still maintaining a good reduction in the carbon footprint.

The possibility of carbon storage in oil fields has also been analyzed, with the aim of reducing the carbon footprint in oil production and decarbonizing onshore industrial activities. In this case, there is a need for a dedicated gas pipeline to transport the CO_2 from the coast to the field where it will be stored. Using the LCA technique for the construction and operation stages, Stewart and Haszeldine [14] evaluated two cases for storing CO_2 from the coast: during the useful life of the field or during part of the useful life. Evidently, the first option can store a greater amount of CO_2, but there is an output of CO_2 that should be stored together with the natural gas associated with the oil. The average values of the emission factors achieved are 0.137 and 0.135 tCO_2e/bbl of oil produced.

Roussanalya et al. [15] evaluated the potential benefits of producing offshore electrical energy on power islands next to natural gas production fields. Using high-efficiency combined cycles and carbon capture systems, the electrical energy produced would be sent to the coast via submarine cables. The authors propose the use of aquifers located close to the oil field for the final disposal of CO_2 so as not to interfere with the production of natural gas. (CO_2 injected into the field diffuses and changes the composition of the natural gas.)

Hydrogen production from natural gas has been proposed. Using the LCA technique, Davies and Hastings [16] evaluated the environmental performance of H_2 production from offshore produced natural gas, with and without CCS, compared to hydrogen production through electrolysis (using only renewable sources or the UK electric grid mix) and against the direct burning of natural gas. For the same annual production of H_2 (2.5 GW/y), gray hydrogen (from natural gas, without CCS) emits 280 MtonCO_2e, and blue hydrogen (from natural gas, with CCS) emits between 200 and 260 MtonCO_2e (depending on CO_2 capture efficiency). Using electrolysis with renewable electrical energy emits 15 MtonCO_2e, and electrolysis using the UK grid emits 165 MtonCO_2e. Directly burning the amount of methane required to produce the defined quantity of H_2 emits 250 MtonCO_2e, less than gray H_2.

3. Description and Operation of the Analyzed Installation

The FPSO analyzed is completely independent from an energy point of view. For topside processes, the electric generation system features four gas turbines with 25 MW of power each, coupled to the main generators of 31 MVA, which generate electrical energy at 13.8 kV. Three generator sets supply electrical energy to the process, and one of them remains as a reserve, even in the situation of maximum electrical load. In addition to this main generation system, there is an auxiliary generator system (in the hull) as well as an emergency generator set. The required process heat comes from cogeneration using the exhaust gases from the gas turbines.

The FPSO production characteristics are presented in Table 1. Figure 2 shows an FPSO similar to the one analyzed in this work.

Table 1. Analyzed FPSO—General Specifications [17].

Characteristic	Maximum Capacity
Liquid processing	24,000 m^3/day
Oil storage	1,600,000 bbl
Oil processing	24,000 m^3/day
Produced water treatment	19,000 m^3/day
Gas treatment and movement	6,000,000 m^3/day
Pressure for natural gas reinjection	55,000 kPa
Pressure for CO_2-rich stream	45,000 kPa
Water injection	28,600 m^3/day

The analysis of CO_2 emissions by the platform takes into account the variation in the quantity and quality of the crude produced by the field over time: the reduction in oil, the increase in gas content, and the increase in the quantity of water that accompanies the oil. Over the time of production (between 25 and 30 years), the properties of the produced fluid change. In particular, CO_2 levels in natural gas can increase significantly. Figure 3 shows a typical production of crude oil until the depletion of the reservoir, simulated by a Weibull statistical distribution, gas-to-oil ratio, oil-to-water ratio, and CO_2 molar fraction in the natural gas.

Figure 2. A FPSO showing the topside processes to produce oil and gas. Source: [18].

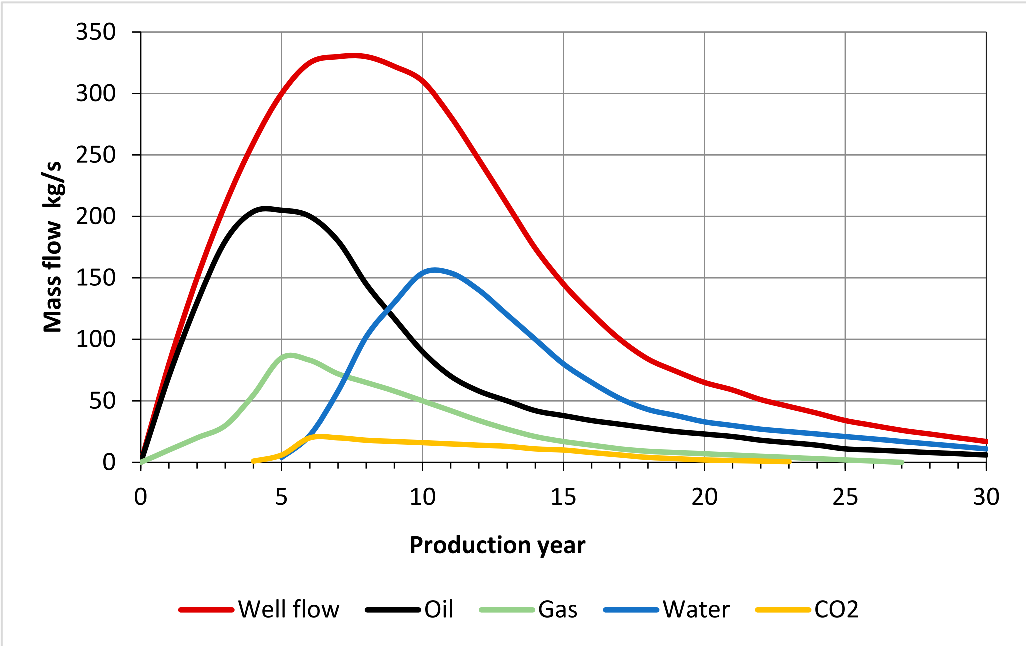

Figure 3. Qualitative shape of a crude oil production curve of an oil field over time.

3.1. Description of the Oil Production and Gas Treatment in the FPSO

A simplified diagram of all topside oil and gas production processes can be seen in Figure 4. The crude oil coming from the wells reaches the production manifold (Box 1) and enters the primary separation process (Box 2).

The oil undergoes treatment to remove residual water and dissolved gases and is sent to the FPSO tanks (black stream). The water separated from the oil goes to a treatment unit that also serves the captured seawater and can be injected into the field's injection wells or discarded (stream in green). The gaseous phase that separated from the oil is sent to the main compression system (Box 4), as well as the resulting gases from the vapor recovery unit (Box 3).

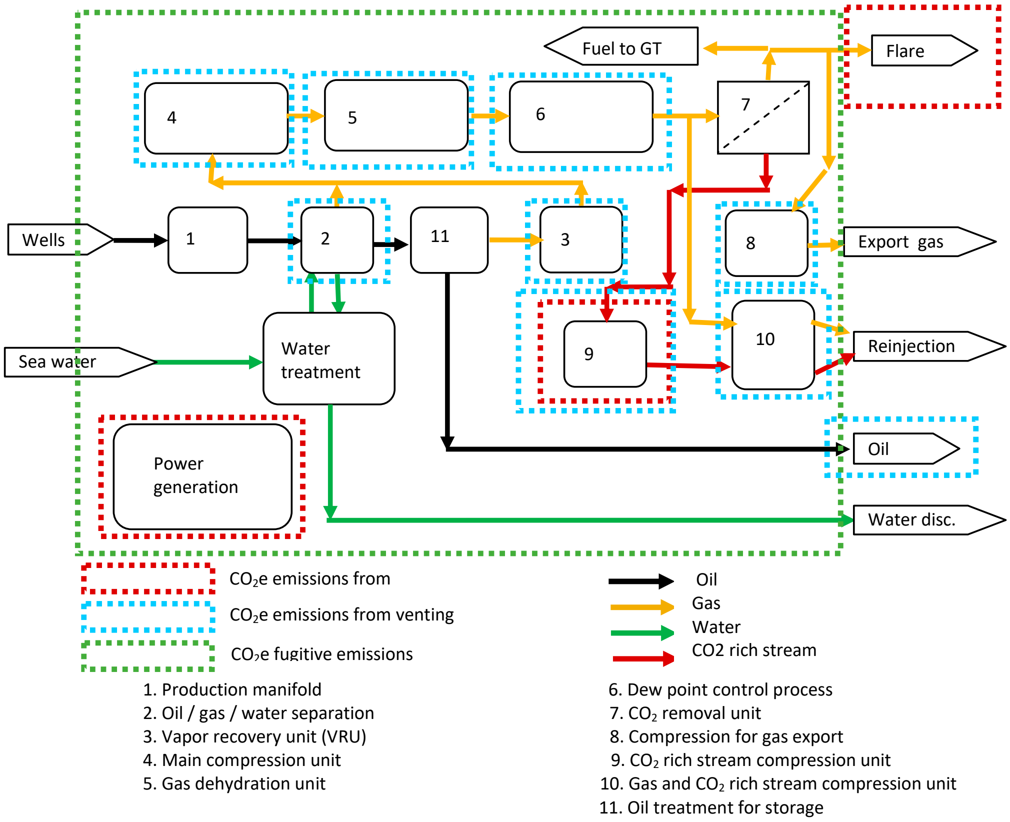

Figure 4. Topside main processes for oil and gas production (simplified).

The gas then passes to the dehydration and dew point control units (Boxes 5 and 6). Depending on the operating condition, the gases are sent to the CO_2 removal unit (Box 7) or sent directly to the gas injection unit (Box 10). If the CO_2 removal unit is operating, the treated gas goes to the gas export unit (Box 8), and the permeate rich in CO_2 (red stream) goes to the CO_2 compression unit (Box 9) and from there to a gas injection unit (Box 10). This last unit can operate with CO_2 or natural gas.

The electrical power required for the processes is provided by three gas turbines, which use locally produced fuel gas whenever possible. CO_2 compressors are driven by dedicated gas turbines; the other compressors and pumps are driven by electric motors.

3.2. The Chosen Operation Conditions of the FPSO

To analyze CO_2 emissions, three typical operating conditions were chosen based on documentation and information from the FPSO project (FEED and PID diagrams). It should be noted that the available data is preliminary, supported by engineering calculations, operational requirements, and various simulations, general aspects of the process, and do not consider data taken from the actual operation.

The design data for the processes related to in oil and gas production involve the following processes and systems: primary separation process; vapor recovery process; natural gas main compression process; gas treatment processes, including dehydration, dew point adjustment, and CO_2 removal unit; gas compression process for export; natural gas compression process for reinjection; CO_2 compression process (injection); electricity and hot water generation system for the FPSO; FPSO utility systems; seawater system; cooling water system; process heating hot water system; diesel oil system; and fuel gas system for use on the platform.

All systems and processes are presented at their maximum capacity settings. However, for each platform operating condition, it is necessary to evaluate each process and system in a combined and coherent way. Thus, simulation models were developed for the partial load operation situation for each type of equipment: oil and gas separators, gas treatment, gas turbines, compressors, pumps, and heat exchangers. The partial load operation models were coupled into the global simulation model.

The global FPSO performance simulation model for each case comprised the conservation of chemical species, conservation of masses, and conservation of energy. To this end, established thermodynamic methodologies and simulation software, such as Aspen HYSYS [19], Thermoflex [20], and EES [21], were used for the different operating cases and calculations of the FPSO platform performance.

The simulation of the topside processes chain was carried out using the Aspen Hysys software, which calculated the mass and energy balances and, in some cases, even the new molar compositions. Gas turbine performance at partial loads was obtained through Thermoflex software.

To carry out the process simulation, two types of virtual equipment were also included: mass flow splitters and mixers. This was necessary because, at various points in the processes, a given mass flow is divided into two or more streams with the same properties, which are sent to different equipment (virtual splitter). Likewise, situations occur in which two or more material streams are mixed (virtual mixer) and not always with the same properties, which generates irreversibility in the process.

The process and utility system simulation model implemented in the ASPEN-HYSYS has a total of 217 pieces of equipment, as shown in Table 2, and a total of 669 material flows connecting equipments.

Table 2. Types and Number of Equipment Considered in the Simulation Model.

Type of Equipment	Quantity
Three-phase separators	3
Two-phase separators	18
Heat exchangers	44
Valves	34
Mass flow splitter (virtual)	42
Mass flow mixers (virtual)	39
Pumps	10
Compressors (including GTs and NG)	17
Combustion chambers (GTs)	5
Turbines (GTs)	5
Total	217

Energy and CO_2 emission diagnoses were prepared for three typical FPSO operating conditions chosen and named as case 7A, case 2B, and case 6A. Such conditions are presented in Table 3 below. It is important to highlight that only the equipment necessary for each case, as well as the relevant material currents, was considered in the simulation. For example, in cases 6 and 7, the CO_2 removal unit and compression system is deactivated, and the associated material streams have zero mass flow rates.

The numbers indicating each case are associated with specific compositions of the natural gas produced before any treatment. Compositions 7, 2, and 6 correspond to CO_2 contents in the natural gas of 12.4%, 25.1%, and 28.3%, respectively, on a molar basis. These high CO_2 molar fractions in the natural gas are typical in the Pre-Salt oil province.

In operating mode A, corresponding to analyzed cases 7 and 6 with different molar fractions in composition, the treated gas goes through a bypass of the CO_2 removal process, and the CO_2 separation unit is inactive. In operating mode B, the gas is sent to the CO_2 removal unit, producing natural gas with a low CO_2 content (<3%) to export, and a CO_2-rich permeate stream, which is sent to the compression unit for re-injection into the oil field.

Table 3. Description of the Operating Conditions in the Diagnosis.

Case	Mode	Oil Field Age
7	A—The CO_2 removal unit is bypassed, and all gas produced must be injected into the oil reservoir.	Max. Oil & Gas
2	B—Treated gas from the CO_2 removal unit is exported; the acidic gas, rich in CO_2, is injected into the oil reservoir.	50% BSW *
6	A—The CO_2 removal unit is bypassed, and all gas produced must be injected into the oil reservoir.	Max. water

* BSW—Basic Sediment and Water.

Case 7A was simulated because it represents a condition of maximum oil and gas. The simulation of this operating condition was based on the primary separation unit. Thus, the other downstream units (vapor recovery and main compression system) received the real mass flows of oil, water, and gas and not the nominal design values. The equipment in these units began to operate at partial loads, as described above. Likewise, each downstream unit received the currents under the real conditions of molar composition and mass flow rate of the unit that preceded it.

Case 2B was simulated because it represents a condition of 50% BSW, which characterizes a period of operation of the field intermediate between the initial condition of maximum oil and gas and the condition of maximum water close to the end of production. This case presents high CO_2 values in crude oil.

Case 6A was simulated because it represents a condition of maximum water, which characterizes a period of field operation close to the end of production. This case also presents high CO_2 values in crude oil.

4. Methodology for Estimating CO_2 Equivalent Emissions

To make the diagnosis of the GHG emissions, equipment classifications were carried out according to the largest sources of emissions in the oil and gas industry [22] presented in Table 4.

Table 4. Classification of the Main Emission Sources.

Category	Main Sources
Direct emissions	
	Emissions from combustion sources: Boilers, heaters, ovens,
Stationary equipment	internal combustion engines, gas turbines, flares, incinerators, etc.
Mobile equipment	Barges, ships, locomotives, trucks, helicopters, airplanes
Process emissions	Amine units, glycol dehydrators, molecular sieves, etc.
Other ventilation sources	Storage tanks, pneumatic devices, chemical injection pumps, flaring, compressor discharge, etc.
Fugitive emission	Valves, flanges, connectors, pumps, compressor leaks, opened lines
Indirect emissions	
Electricity	Off-site electricity generation for on-site consumption
Steam/Heat	Off-site steam and/or process heat production for on-site consumption

According to the emission source, methodologies were developed to approach the emission inventory analysis, as well as numerical approximations to the amounts of GHG released into the atmosphere, using the Global Warming Potential (GWP) as equivalence created by the Intergovernmental Panel on Climate Change (IPCC—a United Nations body for assessing the science related to climate change) [10] in estimating the CO_2 equivalent for the CH_4 emissions (Table 5).

Table 5. GWP Indicator with and without Climate–Carbon Feedback.

Green House Gas	Lifetime (Years)	GWP_{100}	
		With Feedback	Without Feedback
CH_4	12.4	34	28
HFC-134a	13.4	1550	1300
CFC-11	45	5350	4660
N_2O	121	298	265
CF_4	50,000	7350	6630

For the three cases in which the analysis was carried out, the following aspects were considered:

- Electrical load values for the GT electric generation and shaft power GT were obtained through simulation in the Aspen HYSYS® software.
- Ambient temperature conditions at 30 °C, sea level.
- Steady-state operating regime, typical operation for oil field age.
- For fugitive emissions, emissions calculated at equipment level according to the design PID diagrams provided.
- Flow of gas burned in the flare as "Assist Gas" and "pilot" maintained constant for the three simulated cases.
- Flare burning efficiency of 98%. The remaining 2% was considered as vented gas.
- Emissions calculated for the FPSO's oil and gas processing operation, without considering auxiliary operations, such as transporting oil to the continent, movement of helicopters, or logistical support boats.

There are several international agencies with protocols and guidelines for estimating greenhouse gases for different applications and industries with high energy intensity. In particular for oil and gas production processes, there are three documents generally used to calculate emissions and which were used to carry out the analysis presented: (a) 2006 IPCC Guidelines for National Greenhouse Gas Inventories [9]; (b) 2009 API Compendium of Greenhouse Gas Emissions for the Oil and Gas Industry [10]; and 1996 EPA AP-42 Compilation of Air Pollutant Emission Factors, Volume 1: Stationary Point and Area Sources [23].

The IPCC recommendations provide an approach of three levels or tiers for analyzing emissions in activities related to oil and gas (exploration, production, refining, and transport). These approaches range from the use of emission factors based on simple production data, or high-level production statistics, to the use of rigorous estimation techniques involving disaggregated activities and actual plant data.

The methodologies mentioned in the API compendium can be used to estimate GHG emissions in individual projects, entire facilities, or enterprise-wide inventories. The purpose of the analysis, as well as the available data, generally determines the level of detail for the selected approximation.

Lastly, the EPA AP-42 protocol provides emission factors in addition to emissions calculation methodologies that are also described in the API compendium but bring together data taken from the industry on which the reported emission factors are based.

The application of each methodology can lead to different results. Satya et al. [24] evaluated GHG emissions on a platform in Indonesia, comparing the API and IPCC methodology. Based on the API method, the contribution of carbon in the fuel corresponds to 97.15% of total emissions. While using the IPCC method, this contribution is 63.88%. The global inventory calculated by the IPCC is 258.357 tCO_2e, which is 55% higher than the value calculated by the API method (166.204 tCO_2e). The authors observed that the greatest contribution to the divergence between values can be attributed to the differences between the values calculated for fugitive emissions in the production of natural gas using different methods.

4.1. GHG Emissions Due to Combustion

The combustion of a substance containing carbon, hydrogen, and oxygen can be represented by the Equation (1) general reaction. If the complete combustion is assumed, the nitrogen of air and an eventual excess air do not interfere in the CO_2 production:

$$C_xH_yO_z + \left(x + \frac{y}{4} - \frac{z}{2}\right)O_2 \rightarrow (x)CO_2 + \left(\frac{y}{2}\right)H_2O \tag{1}$$

Natural gas is a mixture of different components, with the most part of them containing carbon. But natural gas can also contain nitrogen, CO_2, and other contaminants.

For every mole of carbon in the fuel molecule *j*, one mole of CO_2 is formed. If *xi* is the number of moles of carbon in the molecule *j*, the carbon mass fraction (*WtCj*) in the component *j* of the fuel gas is given by Equation (2):

$$WtC_j = \frac{xi \times 12}{1 \times MW_j}\left[\frac{kgCarbon}{kgsubstancej}\right] \tag{2}$$

The total amount of carbon in the gas mixture is the sum of the contributions to each substance *j* composing the gas mixture, given by Equation (3):

$$WtC_{mixture} = \sum_{j=1}^{comp}\left(Wt_j \times WtC_j\right)\left[\frac{kgCarbon}{kggasmixture}\right] \tag{3}$$

where $WtC_{mixture}$ is the overall mass fraction of carbon in the natural gas and *Wtj* is the mass fraction of the substance *j* in the gas.

Finally, knowing that each mass unit of carbon produces 44/12 mass units of CO_2 and also the fuel mass flow, the CO_2 emission from combustion is given by Equation (4):

$$E_{CO_2} = \frac{\dot{m}_g \times WtC_{mixture} \times 44}{12}\left[\frac{kgCO_2}{s}\right] \tag{4}$$

where $\dot{m}_g$ is the fuel mass flow in kg/s.

For each case analyzed, the composition of the fuel gas is determined by the oil and gas separation and gas treatment processes. Likewise, the simulation of topside processes determines the FPSO's energy demand and the corresponding mass fuel consumption.

Depending on the FPSO's operating mode, two or three gas turbines operate to generate electricity and process heat. The two gas turbines dedicated to driving the compressor for CO_2-rich stream may or may not be in operation. There is no supplemental burning of natural gas in the heat recovery boilers of the cogeneration system.

4.2. Flare GHG Emissions

The flaring process is normally used on offshore platforms to burn gas for emergency procedures, vessel depressurization processes, or other operational or safety reasons. The flare is always burning to cope with rapid operational demands. This burning must be kept as low as possible. The cases studied include the burning in the flare of only gas flows corresponding to the pilot and assistance gas. Knowing the flow rates of gas burned in the flare along with its composition, the flow rates of CO_2 produced were determined using the equations shown above for combustion processes. However, a flare efficiency was considered, with the remainder being released into the atmosphere as unburned gas. Equation (4) was adapted to obtain Equation (5), with the introduction of the term "EC," which is the efficiency for the flare. In the flare, there is a methane slip to atmosphere, a GHG emission worse than the emission of CO_2. This reduces the CO_2 emissions but increases the CH_4 emissions:

$$E_{CO_2} = \frac{\dot{m}_g \times EC \times WtC_{misture} \times 44}{12} \tag{5}$$

where the term *EC* corresponds to the flare efficiency. The flare efficiency was fixed at 98%. The 2% of gas not burned in the flare also contributes to GHG emissions, being counted as vented gas (CH_4).

4.3. Fugitive GHG Emissions

Fugitive emissions are caused by uncontrolled leaks in equipment. Any pressurized equipment can generate leaks, especially in pipes, valves, open lines, and flanges, among others. Table 6 shows the types and quantities of FPSO equipment considered for the fugitive emissions assessment.

Table 6. Count of Equipment to Calculate Fugitive Emissions.

Component	Valve	Pump Seal	Connections	Flanges	Open Lines	Other
Gas composition 1: without CO_2 removal						
Pig 1	45	0	16	54	14	2
Pig 2	49	0	16	54	14	2
Pig 3	37	0	8	36	7	2
Principal manifold	39	0	50	62	2	2
Three-phase separator	30	0	16	38	6	4
Oil dehydrator 1	23	0	8	32	8	2
Oil dehydrator 2	23	0	8	32	8	2
Principal pump	8	0	8	32	8	4
Oil transfer pump	23	6	12	18	8	2
Vapor recovery unit	39	0	12	44	6	2
Knockout drum	32	0	8	30	13	2
Main gas compressors (3 units)	105	0	8	132	9	6
Gas dehydrator system	42	0	8	48	8	2
Dew point control system	148	0	8	214	32	2
Total	665	6	194	846	147	38
Gas composition 2—Treated gas—CO_2 < 3%						
CO_2 removal system	12	0	8	20	4	2
Gas compressor—first stage—to export	105	0	8	66	16	6
Gas compressor—second stage—to export	96	0	8	108	21	6
Exportation gas header	42	0	8	46	5	2
Total	255	0	32	240	46	16
Gas composition 3—CO_2-rich stream						
CO_2 ompressor—first stage	52	0	6	62	9	2
CO_2 compressor—second stage	43	0	6	53	8	2
CO_2 compressor—third stage	36	0	6	44	8	2
CO_2 compressor—fourth stage	46	0	6	56	8	2
CO_2 injection compressor	112	0	8	120	24	2
CO_2 injection header	52	0	8	72	13	4
Total	341	0	40	407	70	14

On an operating platform, there are usually measuring methods and equipment that allow obtaining estimated data on fugitive emissions. For the cases studied, an analysis was performed at the component level, using emission factors reported by the EPA [25] (Table 7), gathered from data reported by the oil and gas industry. It is worth noting that the API also reports emission factors at the component level, which is why they are considered and compared with the EPA factors in the analysis carried out.

Table 7. EPA and API Emission Factors for Fugitive Emissions.

Component	Emission Factor	
	EPA (kg gas/hr/comp.)	API (Ton. TOC/hr/comp.)
Valves	4.50×10^{-3}	5.14×10^{-7}
Pump seals	2.40×10^{-3}	1.95×10^{-7}
Connectors	2.00×10^{-4}	1.08×10^{-7}
Flanges	3.90×10^{-4}	1.97×10^{-7}
Open lines	2.00×10^{-3}	1.01×10^{-6}
Other	8.80×10^{-3}	6.94×10^{-6}

The methodology adopted corresponds to the application of emission factors to an inventory of components, carried out based on information provided by the PID diagrams of the processes and considering the content of CH_4 and CO_2 present in the fuel gas mixture. The general method recommended by the EPA to obtain the total organic compounds (TOC) emissions is as follows:

$$E_{TOC} = FE \times MF_{TOC} \times N \tag{6}$$

for determining emissions of TOC. FE stands for emission factor from Table 7, MF_{TOC} is the mass fraction of the TOC in the gas (assumed = 1 in this work), and N is the number of components, which presents a given FE (example: number of flanges) listed in Table 6.

CH_4 and CO_2 emissions are obtained from their respective mass fractions in total organic carbon emissions:

$$E_{CH_4} = E_{TOC} \times MF_{CH_4} \tag{7}$$

$$E_{CO_2} = E_{TOC} \times MF_{CO_2} \tag{8}$$

4.4. Emissions from Processes and Ventilation

Ventilation emissions correspond to releases of gases into the atmosphere as a product of operational practices or equipment design. For the case studied, emissions from ventilation in the processes of flaring, molecular sieves, flash in the oil storage tank, and others were evaluated.

In the case of the flare, a ventilation of 2% of the gas flow used in the flare was considered. Equations (7) and (8) can be used to calculate the CH_4 and CO_2 flow rates emitted in the process.

Molecular sieves have adsorbent materials, such as zeolites, that have an affinity for water. During the change of material, the gases contained in the sieve vessel are released, which constitute GHG emissions. Emissions are estimated [26,27] according to the internal volume of the dehydrator, as follows:

$$PG = \frac{H^2 \times D^2 \times \pi \times P_2 \times G \times N}{4 \times P_1} \tag{9}$$

where PG is the gas loss; H is the height of the dehydrator; D is the diameter of the dehydrator; P_2 is the gas pressure; P_1 is the atmospheric pressure; G is the fraction of the vessel volume occupied by gas; and N is the number of desiccant changes per year. With the gas mass flow rate, CH_4 and CO_2 emissions can be calculated by Equations (7) and (8).

There are several methodologies to estimate emissions caused by flash processes in storage tanks, where gas contained in oil is released into the atmosphere due to pressure changes between process lines and the tank. The Vasquez–Beggs empirical correlation [28] for gas–oil ratio can be used to estimate the relationship between gas and oil at process conditions and is given by Equation (10):

$$R_s = C_1 \times SG_x \times (P_i + 14.7)^{C_2} \times exp\left(\frac{C_3 \times API}{T_i + 460}\right) \tag{10}$$

where R_s is the gas produced by oil flash in the storage tank (scf/bbl). C1, C2, and C3 are nondimensional coefficients with values given in Table 8. Once the production and composition of the oil stored in the tanks is known, Equations (7) and (8) are employed to calculate the flow rates of methane and carbon dioxide emitted into the atmosphere.

Table 8. Coefficients for Equation (10)—the Vasquez–Begg Calculation of GOR.

Coefficient	API ≤ 30	API > 30
C1	0.0362	0.0178
C2	1.0937	1.1870
C3	25.7240	23.931

The specific weight at 100 psig is necessary data and can be calculated by Equation (11):

$$SG_x = SG_i \times \left[1 + 0.00005912 \times API \times T_i \times log\left(\frac{P_i + 14.7}{114.7}\right)\right] \tag{11}$$

where SGi is the gas-specific gravity at the reference separator pressure and SGi is the gas-specific gravity at the actual separator conditions of Ti (°F) and pi (psig).

Other sources of emission from ventilation, such as purging vessels and compressors, as well as starting compressors, were analyzed using emission factors reported by API.

4.5. Proposed GHG Emissions Indicators

Some GHG emissions indicators were proposed, which can be used for comparisons between different facilities and/or operating regimes. The energy diagnosis of the FPSO operating in different conditions constitutes a baseline for future comparisons. Thus, the indicators can be used to compare different operating strategies of the FPSO in its current design or to compare different proposals for changing processes and/or operating regimes.

Changes in the characteristics of the fluid present in the field, plant operating modes, and field production stage (beginning, end of production in the field, or intermediate situations) can be compared through the emissions indicators.

Indicator 1: ratio of the GHG emissions from GT to electricity produced. This indicator relates the total GHG emissions produced by gas turbine generators to the amount of electrical energy produced and is expressed in kg CO_2e/kWh. It can be used to compare the emissions of different electricity production technologies for the FPSO.

$$Ind1 = \frac{GHG\ emissions\ to\ generate\ electricity}{Produced\ electric\ energy} \tag{12}$$

Indicator 2: Total GHG emissions per useful energy produced. This indicator relates total GHG emissions to the total amount of useful energy produced (electricity and process heat) by the cogeneration system of the FPSO and is expressed in kg CO_2e/TJ.

$$Ind2 = \frac{Total\ GHG\ emissions}{Produced\ energy\ in\ cogeneration[GJ]} \tag{13}$$

Indicator 3: Total GHG emissions per barrel of oil equivalent produced. This indicator relates total GHG emissions to the amount of hydrocarbons produced by the FPSO (oil and gas) expressed in kg CO_2e/BOE:

$$Ind3 = \frac{Total\ GHG\ emissions}{Produced\ BOE(oil\ and\ gas)} \tag{14}$$

5. Results and Discussion

As previously mentioned, the simulation of the oil and gas processing plant was the first step of the methodology, as it allows the obtaining of essential variables for calculating emissions for each case of operation.

5.1. Main Results of the Operation Simulation

Table 9 shows the production data resulting from the simulation, such as the amount of crude oil, the amount of oil exported, exported gas, injected gas, injected rich CO_2 stream, and use of seawater. Given the nominal capacity of the platform, the results make it clear the need to consider partial load operation of each equipment and process.

Table 9. Production Details for the Analyzed Cases.

Description	Mass Flow [kg/s]		
Inlet	**Case 7A**	**Case 2B**	**Case 6A**
Crude oil	311.8	299.3	338.7
Seawater	1480.3	731.2	790.6
Imported fuel gás	5.42	0.0	3.20
Outlet			
Exported oil	212.5	89.0	36.1
Exported gas	0.0	16.8	0.0
Injected gas	92.8	0.0	46.2
Injected rich CO_2 stream	0.0	15.6	0.0
Gas to flare	0.9	0.9	0.9
Water in crude oil	15.9	186.4	268.8
Injected water	338.6	203.7	266.3
Discarded water (sea)	1157.6	713.9	793.1

The performance of the electrical, thermal, and mechanical energy production systems is presented in Table 10. Fuel consumption in each case was used to calculate GHG emissions from combustion.

Table 10. Generation of Power and Heat for the Processes.

	Case 7A	**Case 2B**	**Case 6A**
Electric demand [MW]	72.75	33.38	31.25
Number of TG operating	3	2	2
Gas turbine generators load [%]	98.0	44.7	63.9
CO_2-rich stream compressor demand [MW]	---	6.8	---
Gas turbine (CO_2-rich compression) load [%]	---	43.8	---
Gas turbine (CO_2-rich compression) operating	---	1	---
Heat demand for processes [MW]	47.15	45.78	33.10
Cogeneration efficiency (energy) [%]	57.9	59.3	63.9
Cogeneration efficiency (exergy) [%]	38.6	35.4	36.9

5.2. GHG Emissions Calculated for Each Operating Mode

With data from the thermodynamic simulation of the FPSO operation under the three chosen conditions, it is possible to quantify GHG emissions using the methodology already described. Tables 11–13 show the results obtained for cases 7A, 2B, and 6A, respectively.

The two methods discussed previously were used: API and EPA. The sources of emissions associated with combustion are the most important, by a large margin. Tables 11–13 show that the values obtained by the two methods are similar, except for fugitive emissions, which have high percentage deviations. In any case, the absolute values of these emissions are small compared to other emissions.

The total GHG emissions are higher for the case 7A, since this operation condition requires a large amount of electrical energy.

Table 11. GHG Emissions in Operating Case 7A.

Emission Sources	Ton CO_2 Equiv/Year		
	API	EPA	% Deviation
Gas turbine for electric generation	360,680	360,717	0.01%
Gas turbine for CO_2-rich compressor	0.00	0.00	0.00%
Flare combustion	78,349	78,360	0.01%
Others—Combustion	494	494	0.00%
Venting	11,654	11,654	0.00%
Fugitive emissions	226	975	76.85%
Total	451,404	452,200	0.18%

Table 12. GHG Emissions in Operating Case 2B.

Emission Sources	Ton CO_2/Year		
	API	EPA	% Deviation
Gas turbine for electric generation	107,625	107,619	−0.01%
Gas turbine for CO_2-rich compressor	49,502	49,465	−0.08%
Flare combustion	78,739	78,723	−0.02%
Others—Combustion	494	493.75	0.00%
Venting	10,452	10,452	0.00%
Fugitive emissions	114	482	76.40%
Total	246,926	247,234	0.12%

Table 13. GHG Emissions in Operating Case 6A.

Emission Sources	Ton CO_2/Year		
	API	EPA	% Deviation
Gas turbine for electric generation	189,600	189,628	0.01%
Gas turbine for CO_2-rich compressor	0.00	0.00	0.00%
Flare combustion	78,721	78,731	0.01%
Others—Combustion	494	494	0.00%
Venting	10,021	10,021	0.00%
Fugitive emissions	62	260	76.12%
Total	278,897	279,132	0.08%

5.3. Comparisons of GHG Emissions Between Cases

5.3.1. Combustion Emissions

Emissions due to combustion sources represent between 95% and 97% of total emissions for the processes analyzed on the FPSO platform. In Figure 5, cases are compared according to emissions from combustion in turbogenerators, turbo-compressors, and the portion corresponding to combustion in the flare.

It is noted that the highest emissions correspond to case 7A, where the amount of gas processed is much higher than in the other cases. Compressor loads are the main contributors to high electrical demand in this case. Case 2B is the only one in which CO_2-rich steam compressors operate, corresponding to 21% of total combustion emissions. Flare emissions are similar between all cases; only the composition of the fuel gas burned between operating modes A and B varies. Although case 2B includes the activation of the CO_2 compression set, case 6A presents higher emissions due to the flow of gas treated throughout the process, greater than in case 2B.

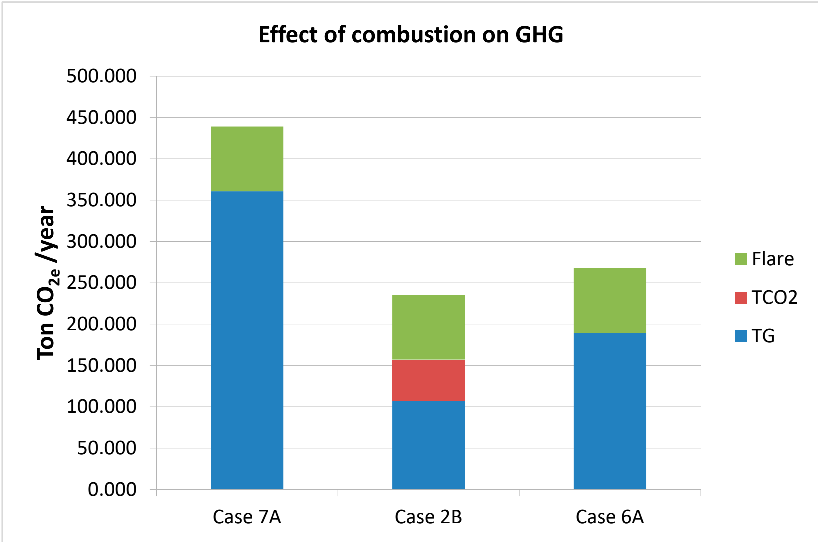

Figure 5. GHG emissions due to combustion. TG is the contribution of turbogenerators, and TC is the contribution of the gas turbine to compress CO_2-rich stream.

5.3.2. Fugitive Emissions

The analysis of fugitive emissions was carried out using emission factors at the level of each component of the FPSO platform. The amount of equipment in the gas pipes in the process was estimated according to data provided, and the emission factors were subsequently applied. When counting equipment, for each case, the number of components used in each subprocess was evaluated, considering the number of compression trains in operation and process segments not in operation in each mode analyzed.

Case 7A treats gas near 80% methane in molar fraction, so the analysis carried out for the entire gas processing in the FPSO points to the highest fugitive emissions in all cases studied, as shown in Figure 6. Case 6A has a high CO_2 content (60% in mole fraction) in the treated gas, meaning emissions are the lowest among the cases studied. This effect is caused by the GHG potential of methane, many times greater than CO_2 itself. Although case 2B has the smallest amount of equipment in operation, emissions are largely affected by the 60% mole fraction composition of methane in the gas produced. The relevance of applying the GWP indicator gives greater importance to emissions due to the treatment of gas with a high CH_4 content, due to the equivalence of the hydrocarbon in relation to CO_2.

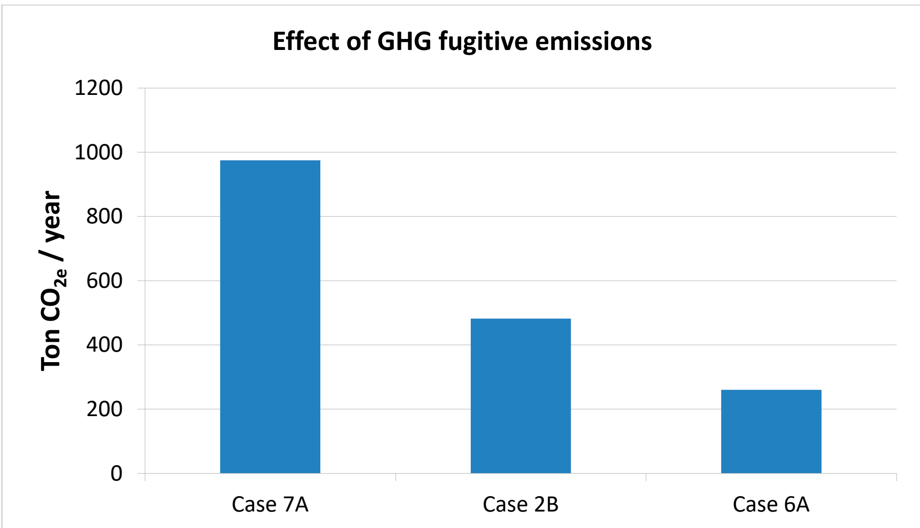

Figure 6. GHG fugitive emissions.

5.3.3. GHG Emissions from Processes and Ventilation

The gas composition is evaluated for each case and for each process described in the methodology, since the ventilation emissions depends on the CH_4 and CO_2 mass fractions in the vented gas. It is expected that ventilation emissions follow a similar behavior to fugitive emissions, since the gas is not burned but rather released into the atmosphere intentionally for operational reasons of the platform or specific equipment. The case that reports the higher ventilation emissions is case 7A, due to the higher percentages of methane in the different types of gas studied, as shown in Figure 7. Although the gas ventilated by the flare corresponds to only 2% of the total gas flow intended for burning in the equipment, it constitutes, on average, 88.6% of total ventilation emissions. Emissions due to molecular sieves for gas treatment and flashing in the FPSO storage tank reach 10.5% of the total and other sources less than 1% (vessel and compressor purges, compressor start-up operations).

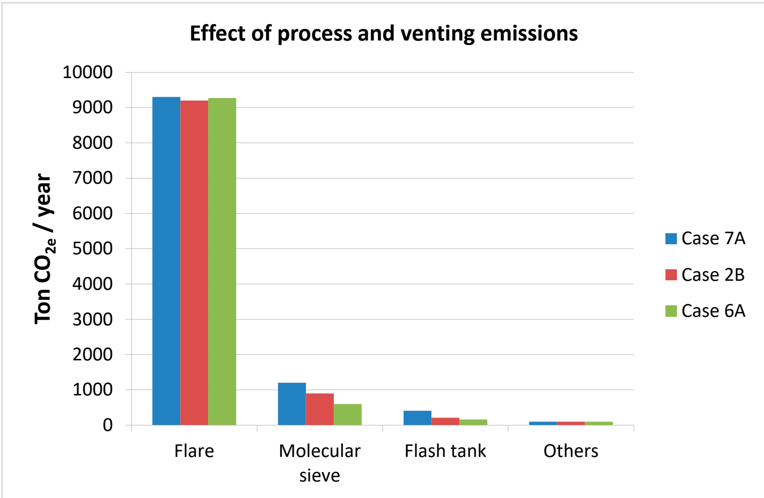

Figure 7. GHG emissions from processes and ventilation.

5.3.4. Overall GHG Emissions

The analysis covers all FPSO operations in the oil and gas production, treatment, and export processes. As previously shown in process emissions, combustion emissions represent in the cases studied between 95% and 98% of the platform's total emissions, as indicated in Figure 8. Therefore, actions to reduce CO_2 in exhaust gases can have major global impacts on emissions.

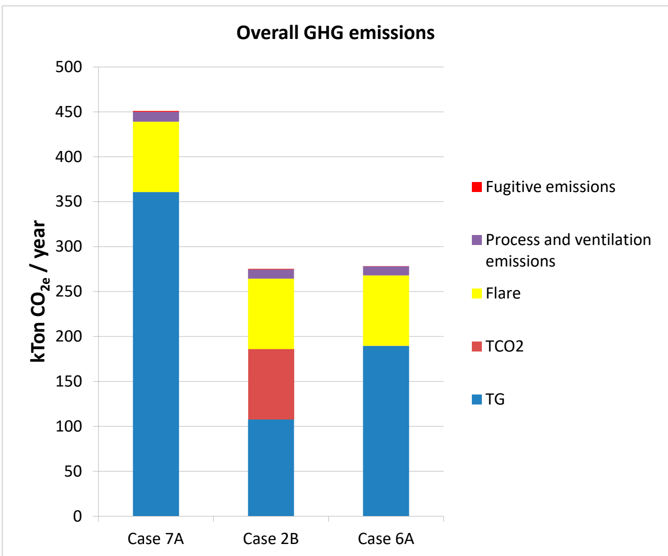

Figure 8. Overall GHG emissions.

5.3.5. GHG Emission Indicators

The first indicator (Table 14) seeks to quantify CO_2 emissions from turbogenerators in relation to the electrical energy produced (Ind1). When operating at lower loads, the turbogenerators in cases 2B and 6A emit more GHG compared with the power generated. This is an effect of the lower gas turbine efficiencies running on partial loads.

Table 14. GHG Emission Indicators.

Units	Case 6A	Case 2B	Case 7A	Emission Indicator	
kg CO_2/kWh	0.655	0.664	0.574	Ratio of GHG emissions from electricity generation to power produced.	Ind 1
kg CO_2/GJ	267.9	290.3	199.9	Ratio of GHG emissions from cogeneration to energy produced (heat and power)	Ind 2
kg CO_2/BOE	171.5	65.2	43.8	Ratio of overall GHG emissions to overall hydrocarbons produced (oil and gas)	Ind 3

Indicator 2 relates total GHG emissions to the total energy produced in the FPSO in TJ (Ind2) and is a measure of the FPSO cogeneration system efficiency. To be noted, the total energy produced is the sum of electric power with the exergy of the process heat. Case 2B is the worse case, due to the large amount of heating water and also to the composition of gas produced, which contains a high level of CO_2. The CO_2-rich stream must be injected into the reservoir, and its compressor is driven by a gas turbine, increasing the fuel consumption.

The indicator that relates the amount of hydrocarbon produced on the platform (Ind3) is not favorable for case 6A, where the flow of crude is high, but the amount of oil produced is small, due to the large amount of water in the crude oil. In case 7, on the contrary, the emission indicator is low due to the high quantity of oil produced (146,000 barrels/day, approximately), and in addition, the gas produced is rich in methane.

6. Conclusions

Given the predominance of combustion processes in GHG emissions in FPSO, it is essential to increase the efficiency of prime movers used for electrical generation or mechanical power. It is recommended to use high-efficiency power systems, such as combined cycles. Therefore, increasing efficiency in electrical generation can represent an important step toward increasing the efficiency of the global production process, with a consequent reduction in CO_2 emissions. Process heat production must also be based on waste heat recovery (WHR) and cogeneration, avoiding gas burning.

The results obtained in quantifying GHG emissions, expressed in terms of CO_2 equivalent, should also be highlighted. Emissions associated with production processes and equipment (ventilation, fugitive) are low when compared to those arising from combustion processes, whether from TGs or the gas turbine that drives the CO_2 compressors or from burning in flare.

The proposed indicators can help establish a baseline from which proposed changes to the project, processes, or operational strategies can be compared.

Author Contributions: Conceptualization, methodology, validation, formal analysis, data curation: V.L.A.B. and W.L.R.G. Software and investigation: V.L.A.B. Resources, writing—review and editing: W.L.R.G. All authors have read and agreed to the published version of the manuscript.

Funding: This study was part of a research project funded by BG Group (now part of Shell Group).

Data Availability Statement: The original data was obtained during a research project with privacy clauses. To access the data, please contact the authors.

Conflicts of Interest: Author Victor Leonardo Acevedo Blanco was employed by the company Vanti Group. The remaining authors declare that the research was conducted in the absence of any commercial or financial relationships that could be construed as a potential conflict of interest.

References

1. IPCC, Intergovernmental Panel on Climate Change. *Climate Change 2013, The Physical Basis. Working group I Contribution to the Fifth Assessment Report of the IPCC*; Cambridge University Press: Cambridge, UK; New York, NY, USA, 2013; 1535p.
2. IEA, International Energy Agency. *Energy and Climate Change, Preserving the Global Environment: The Challenge of Shared Leadership*; IEA: Paris, France, 2014.
3. ANP, Agência Nacional do Petróleo [Brazilian Agency for Oil, Natural Gas and Biofuels]. *Oil, Natural Gas and Biofuels Statistical Yearbook*; ANP: Rio de Janeiro, RJ, Brazil, 2023.
4. ANP. Agência Nacional do Petróleo, Gás Natural e Biocombustíveis, Boletim Mensal da Produção de Óleo e Gás. Maio de 2024. (Brazilian Agency for Oil, Natural Gas and Biofuels. Oil and Gas Monthly Bulletin, May 2024). 2024. Available online: https://www.gov.br/anp/pt-br/centrais-de-conteudo/publicacoes/boletins-anp/boletins/arquivos-bmppgn/2024/maio.pdf (accessed on 30 July 2024). (In Portuguese)
5. Barreira, J.E.; Sahlit, A.A.; Bazzo, E. Exergy analysis and strategies for the waste heat recovery in offshore platforms. In Proceedings of the 22th International Congress of Mechanical Engineering (COBEM 2013), Ribeirão Preto, SP, Brazil, 3–7 November 2013.
6. De Oliveira, S., Jr.; Sanchez, Y.A.C. Exergy Analysis of Petroleum Offshore Platform Process Plant with CO_2 Capture. In Proceedings of the 27th International Conference on Efficiency, Cost, Optimization, Simulation and Environmental Impact of Energy Systems (ECOS 2014), Turku, Finland, 15–19 June 2014; pp. 1–15.
7. De Oliveira Jr, S.; Van Hombeeck, M. Exergy analysis of petroleum separation processes in the offshore platforms. *Energy Convers. Manag.* **1997**, *38*, 1577–1584. [CrossRef]
8. Rivero, R. Application of the exergy concept in the petroleum refining and petrochemical industry.(Keynote paper). *Energy Convers. Manag.* **2002**, *43*, 1199–1220. [CrossRef]
9. IPCC, Intergovernmental Panel on Climate Change. *2006 IPCC Guidelines for National Greenhouse Gas Inventories*; Volume 2: Energy; IGES: Hayama, Japan, 2006.
10. Shires, T.M.; Loughran, C.J.; Jones, S.; Hopkins, E. *Compendium of Greenhouse Gas Emissions Methodologies for the Oil and Natural Gas Industry*; API: Washington, DC, USA, 2009; pp. 1–807.
11. Silva, J.A.M.; De Oliveira, S., Jr. Unit exergy cost and CO_2 emissions of offshore petroleum production. *Energy* **2018**, *147*, 757–766. [CrossRef]
12. Voldsund, M.; Reyes-Lúa, A.; Fu, C.; Ditaranto, M.; Nekså, P.; Mazzetti, M.J.; Brekke, O.; Bindingsbø, A.U.; Grainger, D.; Pettersen, J. Low carbon power generation for offshore oil and gas production. *Energy Convers. Manag. X* **2023**, *17*, 100347. [CrossRef]
13. Li, Z.; Zhang, H.; Meng, J.; Long, Y.; Yan, Y.; Li, M.; Huang, Z.; Liang, Y. Reducing carbon footprint of deep-sea oil and gas field exploitation by optimization for Floating Production Storage and Offloading. *Appl. Energy* **2020**, *261*, 114398. [CrossRef]
14. Stewart, R.J.; Haszeldine, R.S. Can Producing Oil Store Carbon? Greenhouse Gas Footprint of CO_2EOR, Offshore North Sea. *Environ. Sci. Technol.* **2015**, *49*, 5788–5795. [CrossRef] [PubMed]
15. Roussanalya, S.; Aasena, A.; Anantharamana, R.; Danielsenb, B.; Jakobsena, J.; Heme-De-Lacottec, L.; Nejic, G.; Sodalb, A.; Wahla, P.E.; Vranaa, T.K.; et al. Offshore power generation with carbon capture and storage to decarbonise mainland electricity and offshore oil and gas installations: A technoeconomic analysis. *Appl. Energy* **2019**, *233–234*, 478–494. [CrossRef]
16. Davies, A.J.; Hastings, A. Lifetime greenhouse gas emissions from offshore hydrogen production. *Energy Rep.* **2023**, *10*, 1538–1554. [CrossRef]
17. Brasil Engenharia. Available online: http://www.brasilengenharia.com/portal/noticias/destaque/11234-casco-da-plataforma-p-66-chega-a-angra-dos-reis (accessed on 15 June 2024). (In Portuguese)
18. Petrobras. 2023. Available online: https://epbr.com.br/petrobras-p-71-o-ultimo-fpso-replicante-atinge-capacidade-maxima-no-pre-sal/ (accessed on 12 July 2024). (In Portuguese)
19. Aspen Technology Inc. *Aspen HYSYS*; Aspen Technology: Burlington, VT, USA, 2015.
20. Thermoflow Inc. *Thermoflex*; Thermoflow Inc.: Southborough, MA, USA, 2015.
21. F-CHART SOFTWARE. EES—Engineering Equation Solver for Microsoft Windows Operating Systems. 2015. Available online: https://fchartsoftware.com/ees/eesoverview/?gad_source=1&gclid=Cj0KCQjwveK4BhD4ARIsAKy6pMLzbmwQ0XMoAtR42HUu93rl7weSNm_3esU030gYJWAy6NXJSfqK2ZUaAqbMEALw_wcB (accessed on 30 July 2024).
22. Gomez, D.R.; Watterson, J.D.; Americanohia, B.B.; Ha, C.; Marland, G.E.; Matsika, G.L.; Namayanga, G.; Osman-Elasha, B.; Saka, J.D.K.; Treanton, K. Chapter 2 Stationary Combustion. In *IPCC Guidelines for National Greenhouse Gás Inventory*; IGES: Hayama, Japan, 2006.
23. EPA, U.S. *Environmental Protection Agency. AP-42 Compilation of Air Pollutant Emission Factors. Volume I: Stationary Point and Area Sources*, 5th ed.; Office of Air Quality: Research Triangle Park, NC, USA, 1995.
24. Satya, P.; Karuniasa, M.; Abdini, C. Estimating GHG Emission Level from Oil and Gas Offshore Production Facility. *E3S Web Conf.* **2020**, *202*, 09004. [CrossRef]
25. EPA, U.S. *Environmental Protection Agency. Protocol for Equipment Leak Emissions Estimates*; *EPA-453/R-95-017*; Office of Air Quality: Research Triangle Park, NC, USA, 1995.

26. EPA. *Replacing Glycol Dehydrators with Desiccant Dehydrators*; Environmental Protection Agency: Washington, DC, USA, 2006; pp. 1–14.
27. OK DEQ. *Calculation of Flashing Losses/VOC Emissions from Hydrocarbon Storage Tanks*; Oklahoma Department of Environmental Quality: Oklahoma City, OK, USA, 2012; pp. 1–10.
28. Ahmed, T. *Reservoir Engineering Handbook*, 4th ed.; Gulf Professional Publishing: Houston, TX, USA, 2010; Chapter 2.